Electronic Supplementary Information (ESI)

Overcoming the interfacial challenges of Ni-rich layered oxide cathodes for all-solid-state batteries through ultrathin and amorphous Al_2O_3 coating

Hun Shim‡[a], Hyun-seung Kim‡[b], Jae Yup Jung[b], Kyeong-Ho Kim[c], Hyung-Ho Kim[a], Eungjae Lee[a], Dongjun Lee[a], Woosuk Cho[b]*, and Seong-Hyeon Hong[a]*

[a] Department of Materials Science and Engineering and Research Institute of Advanced Materials, Seoul National University, Seoul 08826, Republic of Korea.

[b] Advanced Batteries Research Center, Korea Electronics Technology Institute, Gyeonggi 13509, Republic of Korea.

[c] Department of Materials Science and Engineering, Pukyong National University, Busan 48513, Republic of Korea.

‡ The first and second authors contributed equally to this work.

* Corresponding author
Dr. Woosuk Cho (W. Cho)
E-mail: cho4153@keti.re.kr

Prof. Seong-Hyeon Hong (S.-H. Hong)
E-mail: shhong@snu.ac.kr

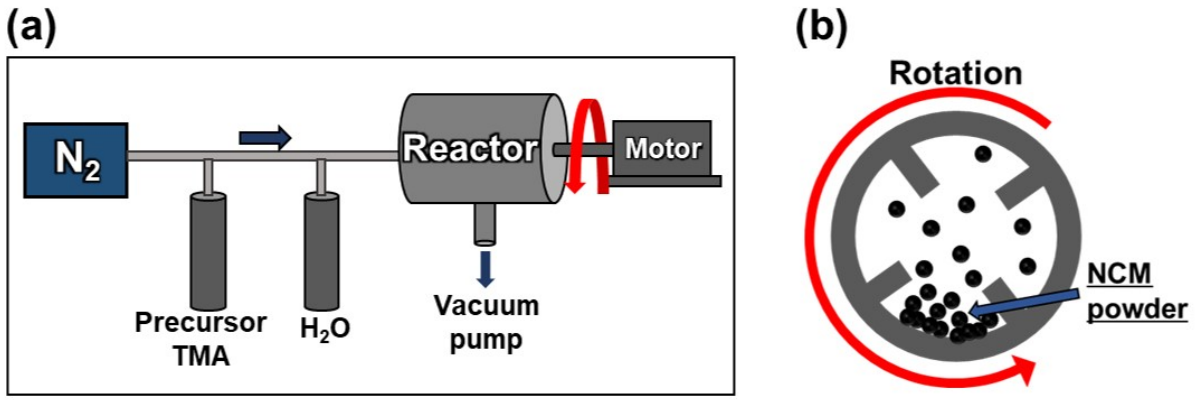

Fig. S1. Schematic illustration of a) powder ALD system and b) cross-section view of the reaction chamber.

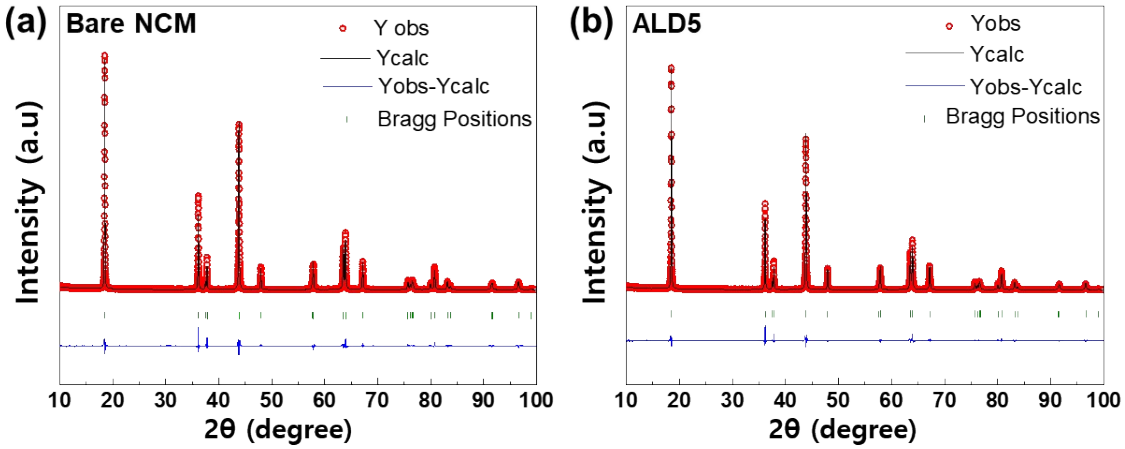

Fig. S2. Result profiles after Rietveld refinement for as-synthesized a) bare NCM and b) ALD5 cathode powders.

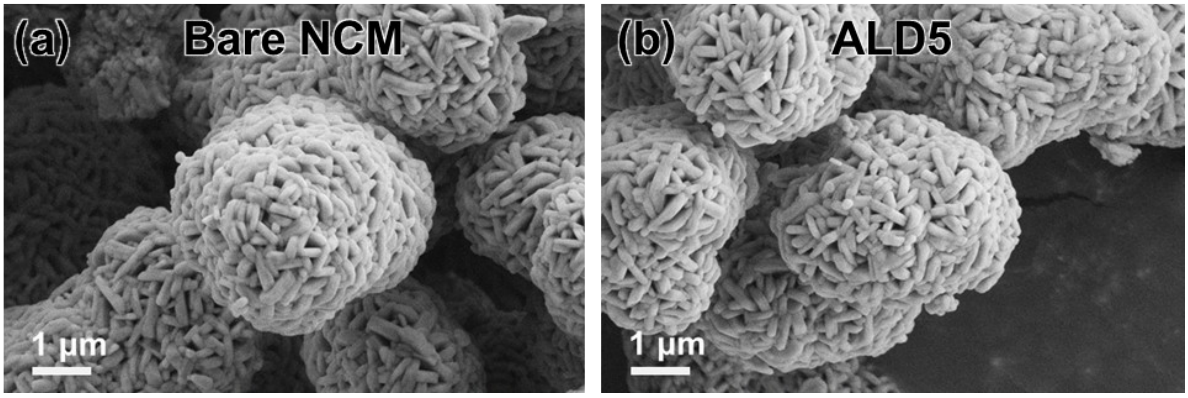

Fig. S3. SEM images of as-synthesized a) bare NCM and b) ALD5 cathode powders.

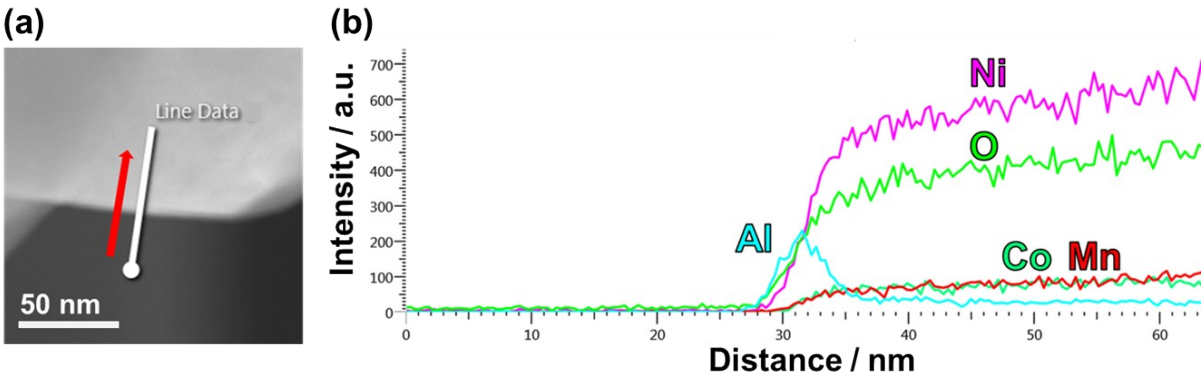

Fig S4. a) High magnification TEM image of as-synthesized ALD5 powder and b) elemental distribution obtained by the EDS line scan along the white line shown in a).

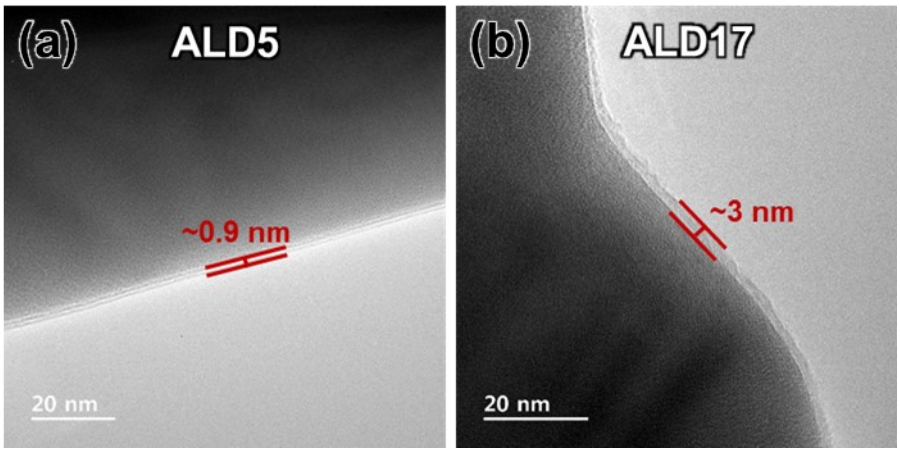

Fig S5. TEM images of as-synthesized a) ALD5 and b) ALD17 powder.

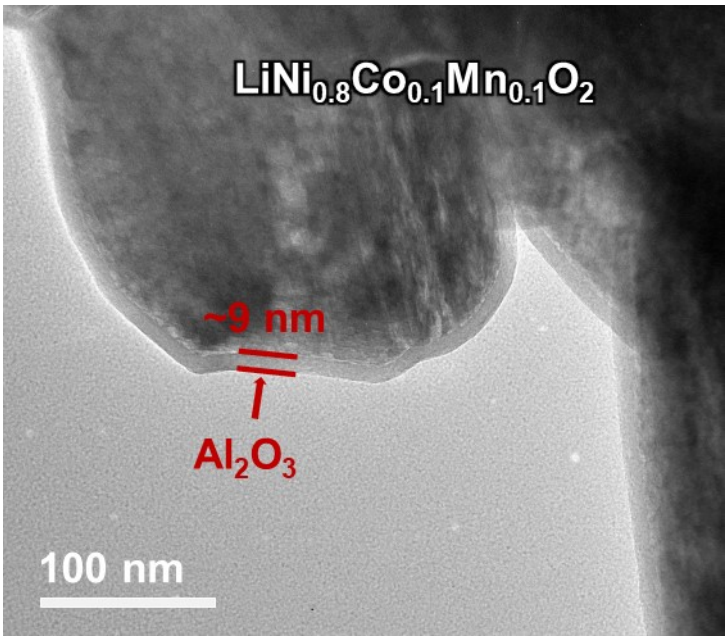

Fig. S6. Low magnification TEM image of as-synthesized ALD50 powder.

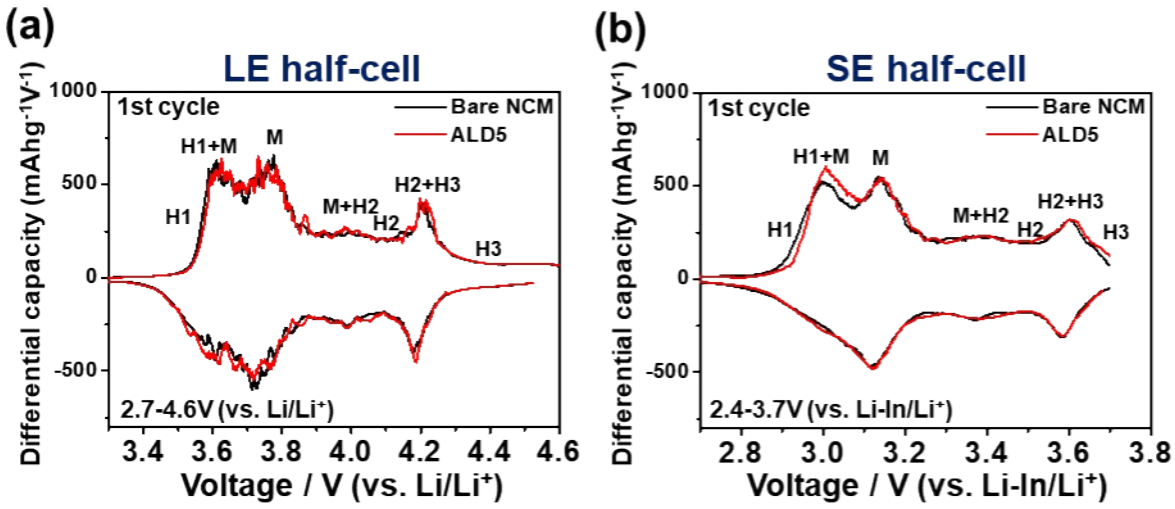

Fig. S7. Differential capacity (dQ dV^{-1}) profiles obtained by differentiating the initial charge-discharge voltage profiles of bare NCM and ALD5 electrodes in a) LE half-cells and b) SE half-cells.

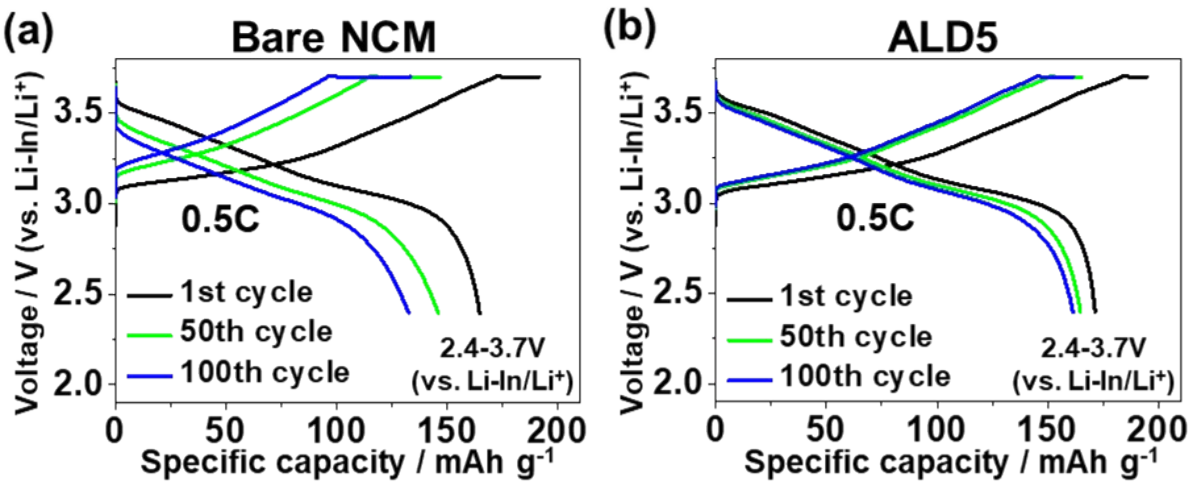

Fig. S8. Initial charge–discharge voltage profiles for 1st, 50th, and 100th cycles of a) bare NCM and b) ALD5 electrodes at the current density of 0.5 C CC-CV between 2.4 and 3.7 V (vs. Li-In/Li^+) at 25 ^oC in SE half-cells.

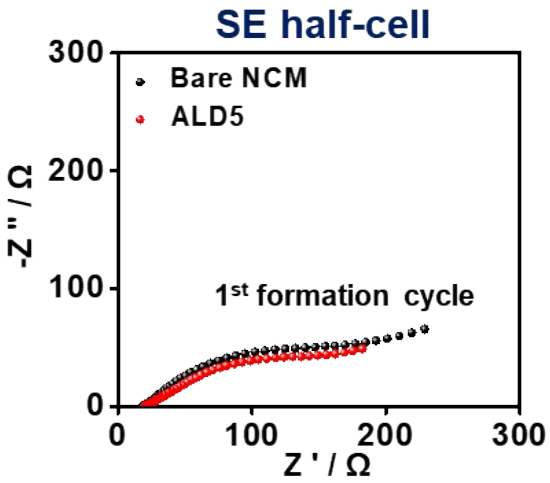

Fig. S9. Nyquist plots for bare NCM and ALD5 electrodes after 1st cycle in SE half-cells (the cells were discharged to 3.7 V (vs. Li-In/Li^+) for the EIS measurement).

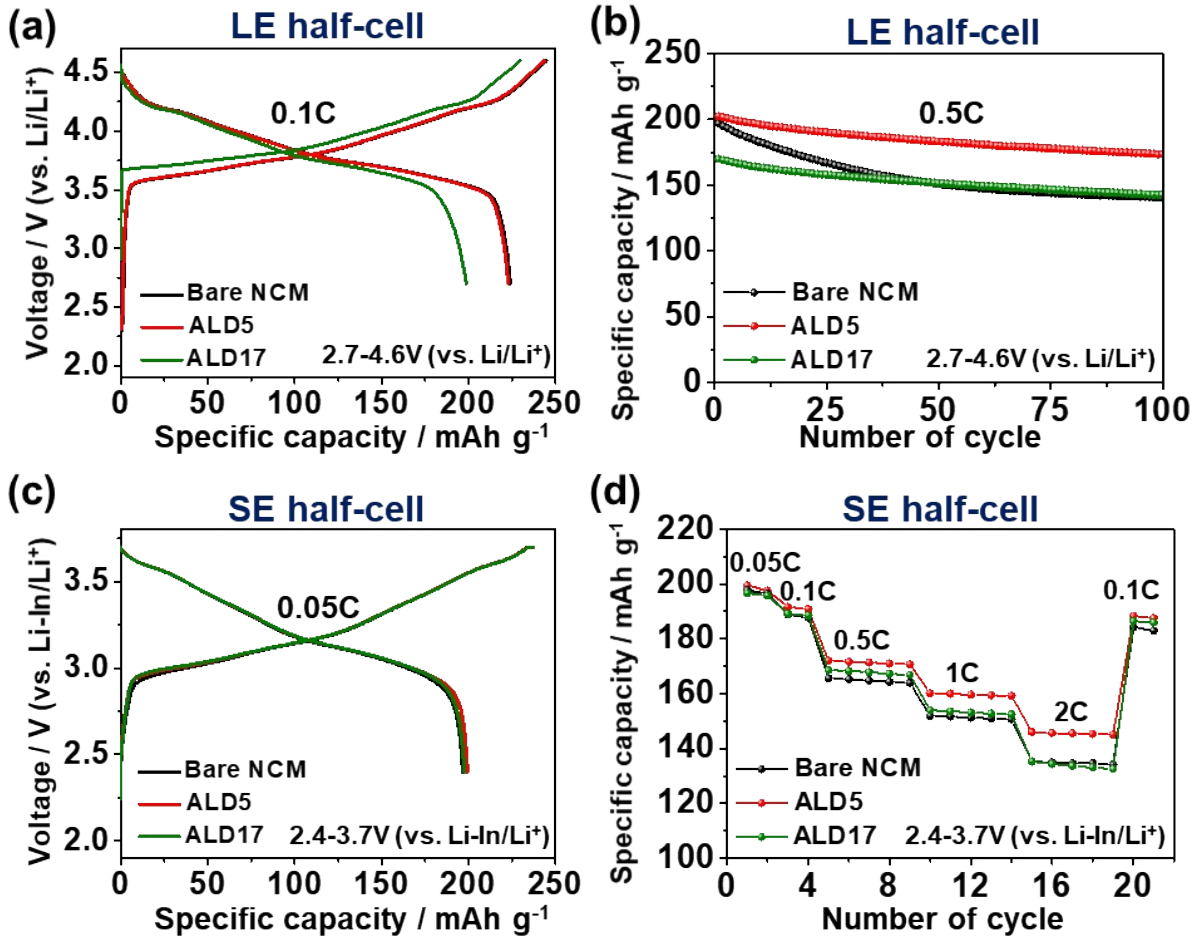

Fig. S10. a) Initial charge–discharge voltage profiles at the current density of 0.1 C, b) cycle performance at the current density of 0.5 C for bare NCM, ALD5, and ALD17 electrodes between 2.7 and 4.6 V (vs. Li/Li^+) at 25 °C in LE half-cells, c) initial charge–discharge voltage profiles at the current density of 0.05 C, d) rate test for bare NCM, ALD5, and ALD17 electrodes between 2.4 and 3.7 V (vs. $Li\text{-}In/Li^+$) at 25 °C in SE half-cells.

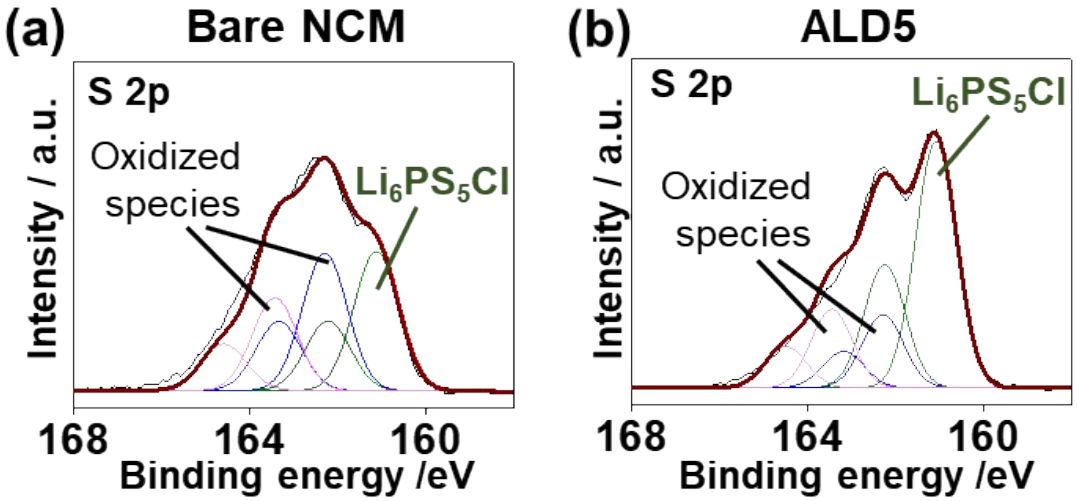

Fig. S11. Deconvoluted S 2p spectra of a) bare NCM and b) ALD5 after evaluation of their cycle performance in SE half-cells.

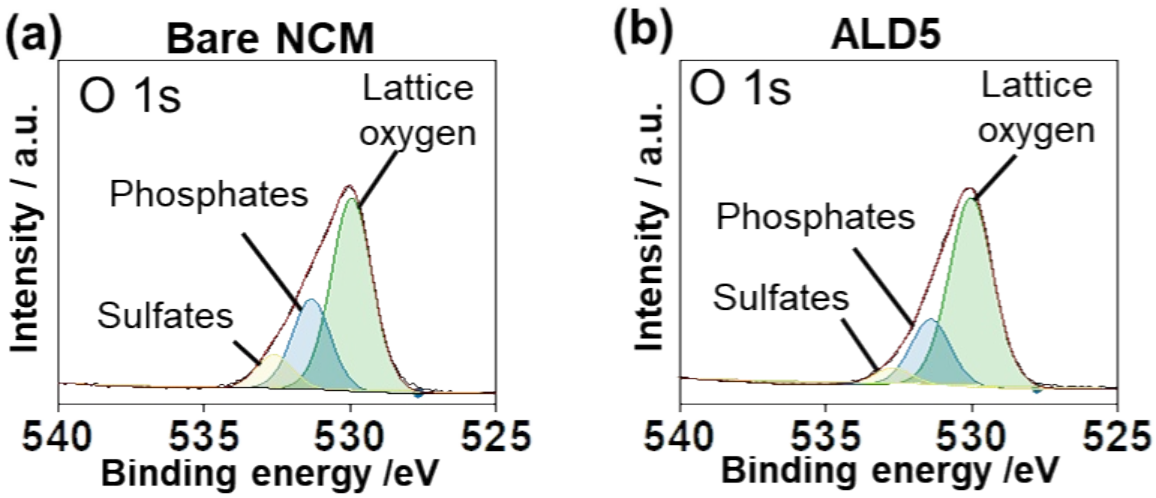

Fig. S12. Ex situ XPS O 1s spectra of a) bare NCM and b) ALD5 after evaluation of their cycle performance in dry-electrode cells.

Table S1. Rietveld refinement results for as-synthesized bare NCM and ALD5 cathode powders.

Sample	a-axis [Å]	c-axis [Å]	c/a	V $[Å]^3$
Bare NCM	2.874	14.205	4.942	101.609
ALD5	2.875	14.204	4.941	101.673